

## 2.2. SINGLE-CRYSTAL X-RAY TECHNIQUES

## 2.2.3. Rotation/oscillation geometry

The main modern book dealing with the rotation method is that of Arndt & Wonacott (1977).

## 2.2.3.1. General

The purpose of the monochromatic rotation method is to stimulate a reflection fully over its rocking width *via* an angular rotation. Different refl's are rotated successively into the reflecting position. The method, therefore, involves rotation of the sample about a single axis, and is used in conjunction with an area detector of some sort, *e.g.* film, electronic area detector or image plate. The use of a repeated rotation or oscillation, for a given exposure, is simply to average out any time-dependent changes in incident intensity or sample decay. The overall crystal rotation required to record the total accessible region of reciprocal space for a single crystal setting, and a detector picking up all the diffraction spots, is  $180^\circ + 2\theta_{\max}$ . If the crystal has additional symmetry, then a complete asymmetric unit of reciprocal space can be recorded within a smaller angle. There is a blind region close to the rotation axis; this is detailed in Subsection 2.2.3.5.

## 2.2.3.2. Diffraction coordinates

Figs. 2.2.3.1(a) to (d) are taken from *IT II* (1959, p. 176). They neatly summarize the geometrical principles of reflection, of a monochromatic beam, in the reciprocal lattice for the general case of an incident beam inclined at an angle ( $\mu$ ) to the equatorial plane. The diagrams are based on an Ewald sphere of unit radius.

With the nomenclature of Table 2.2.3.1: Fig 2.2.3.1(a) gives

$$\sin \nu = \sin \mu + \zeta. \quad (2.2.3.1)$$

Fig. 2.2.3.1(b) gives, by the cosine rule,

$$\cos \Upsilon = \frac{\cos^2 \nu + \cos^2 \mu - \xi^2}{2 \cos \nu \cos \mu} \quad (2.2.3.2)$$

and

$$\cos \tau = \frac{\cos^2 \mu + \xi^2 - \cos^2 \nu}{2 \xi \cos \mu}, \quad (2.2.3.3)$$

and Figs. 2.2.3.1(a) and (b) give

$$\xi^2 + \zeta^2 = d^{*2} = 4 \sin^2 \theta. \quad (2.2.3.4)$$

The following special cases commonly occur:

(a)  $\mu = 0$ , normal-beam rotation method, then

$$\sin \nu = \zeta \quad (2.2.3.5)$$

and

$$\cos \Upsilon = \frac{2 - \xi^2 - \zeta^2}{2\sqrt{1 - \zeta^2}}; \quad (2.2.3.6)$$

(b)  $\mu = -\nu$ , equi-inclination (relevant to Weissenberg upper-layer photography), then

$$\zeta = -2 \sin \mu = 2 \sin \nu \quad (2.2.3.7)$$

$$\cos \Upsilon = 1 - \frac{\xi^2}{2 \cos^2 \nu}; \quad (2.2.3.8)$$

(c)  $\mu = +\nu$ , anti-equi-inclination

$$\zeta = 0 \quad (2.2.3.9)$$

$$\cos \Upsilon = 1 - \frac{\xi^2}{2 \cos^2 \nu}; \quad (2.2.3.10)$$

(d)  $\nu = 0$ , flat cone

$$\zeta = -\sin \mu \quad (2.2.3.11)$$

$$\cos \Upsilon = \frac{2 - \xi^2 - \zeta^2}{2\sqrt{1 - \zeta^2}}. \quad (2.2.3.12)$$

In this section, we will concentrate on case (a), the normal-beam rotation method ( $\mu = 0$ ). First, the case of a plane film or detector is considered.

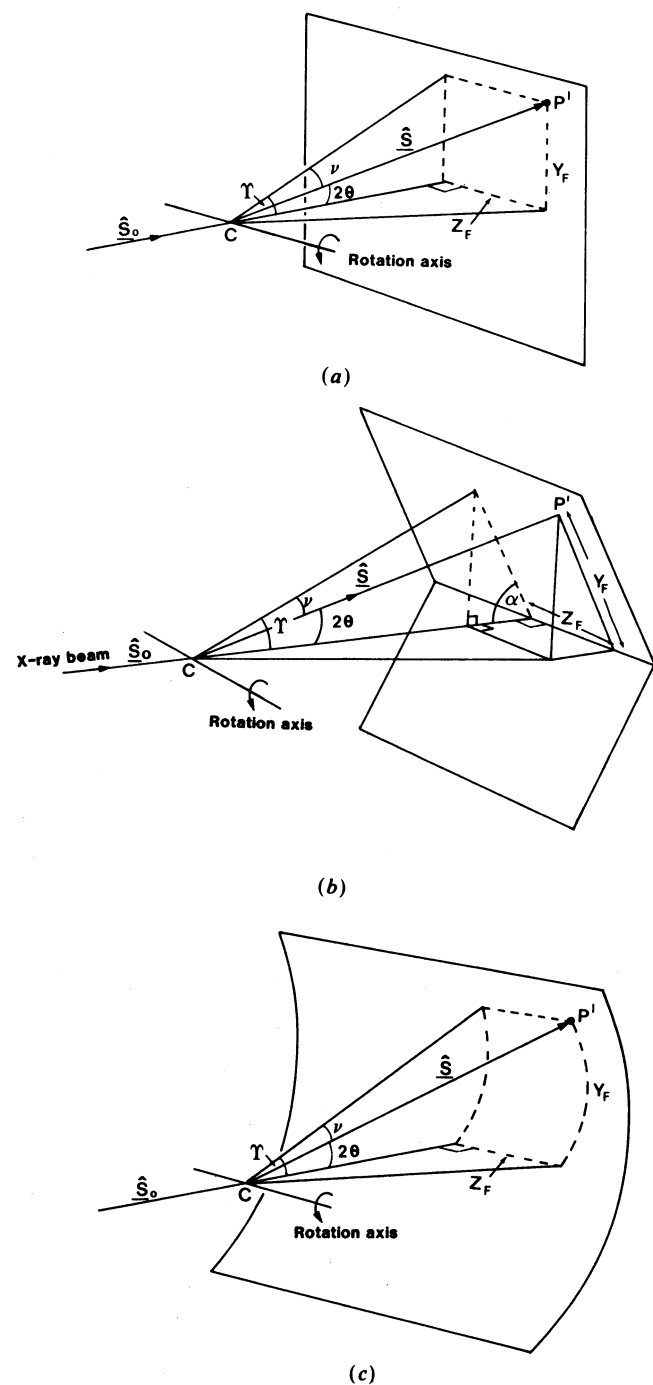


Fig. 2.2.3.2. Geometrical principles of recording the pattern on (a) a plane detector, (b) a V-shaped detector, (c) a cylindrical detector.

## 2. DIFFRACTION GEOMETRY AND ITS PRACTICAL REALIZATION

Table 2.2.3.1. *Glossary of symbols used to specify quantities on diffraction patterns and in reciprocal space*

$\theta$	Bragg angle
$2\theta$	Angle of deviation of the reflected beam with respect to the incident beam
$\hat{S}_o$	Unit vector lying along the direction of the incident beam
$\hat{S}$	Unit vector lying along the direction of the reflected beam
$s = (\hat{S} - \hat{S}_o)$	The scattering vector of magnitude $2 \sin \theta$ . $s$ is perpendicular to the bisector of the angle between $\hat{S}_o$ and $\hat{S}$ . $s$ is identical to the reciprocal-lattice vector $\mathbf{d}^*$ of magnitude $\lambda/d$ , where $d$ is the interplanar spacing, when $\mathbf{d}^*$ is in the diffraction condition. In this notation, the radius of the Ewald sphere is unity. This convention is adopted because it follows that in Volume II of <i>International Tables</i> (p. 175). Note that in Section 2.2.1 <i>Laue geometry</i> the alternative convention ( $ \mathbf{d}^*  = 1/d$ ) is adopted whereby the radius of each Ewald sphere is $1/\lambda$ . This allows a nest of Ewald spheres between $1/\lambda_{\max}$ and $1/\lambda_{\min}$ to be drawn
$\zeta$	Coordinate of a point $P$ in reciprocal space parallel to a rotation axis as the axis of cylindrical coordinates relative to the origin of reciprocal space
$\xi$	Radial coordinate of a point $P$ in reciprocal space; that is, the radius of a cylinder having the rotation axis as axis
$\tau$	The angular coordinate of $P$ , measured as the angle between $\xi$ and $\hat{S}_o$ [see Fig. 2.2.3.1(b)]
$\varphi$	The angle of rotation from a defined datum orientation to bring a relp onto the Ewald sphere in the rotation method (see Fig. 2.2.3.3)
$\mu$	The angle of inclination of $\hat{S}_o$ to the equatorial plane
$\gamma$	The angle between the projections of $\hat{S}_o$ and $\hat{S}$ onto the equatorial plane
$\nu$	The angle of inclination of $\hat{S}$ to the equatorial plane
$\omega, \chi, \varphi$	The crystal setting angles on the four-circle diffractometer (see Fig. 2.2.6.1). The $\varphi$ used here is not the same as that in the rotation method (Fig. 2.2.3.3). This clash in using the same symbol twice is inevitable because of the widespread use of the rotation camera and four-circle diffractometer.

The equatorial plane is the plane normal to the rotation axis.

The notation now follows that of Arndt & Wonacott (1977) for the coordinates of a spot on the film or detector.  $Z_F$  is parallel to the rotation axis and  $\zeta$ .  $Y_F$  is perpendicular to the rotation axis and the beam. *IT II* (1959, p. 177) follows the convention of  $y$  being parallel and  $x$  perpendicular to the rotation-axis direction, *i.e.*  $(Y_F, Z_F) \equiv (x, y)$ . The advantage of the  $(Y_F, Z_F)$  notation is that the  $x$ -axis direction is then the same as the X-ray beam direction.

The coordinates of a reflection on a flat film  $(Y_F, Z_F)$  are related to the cylindrical coordinates of a relp  $(\xi, \zeta)$  [Fig. 2.2.3.2(a)] by

$$Y_F = D \tan \gamma \quad (2.2.3.13)$$

$$Z_F = D \sec \gamma \tan \nu, \quad (2.2.3.14)$$

which becomes

$$Z_F = 2D\zeta/(2 - \xi^2 - \zeta^2), \quad (2.2.3.15)$$

where  $D$  is the crystal-to-film distance.

For the case of a V-shaped cassette with the V axis parallel to the rotation axis and the film making an angle  $\alpha$  to the beam direction [Fig. 2.2.3.2(b)], then

$$Y_F = D \tan \gamma / (\sin \alpha + \cos \alpha \tan \gamma) \quad (2.2.3.16)$$

$$Z_F = (D - Y_F \cos \alpha) \zeta / (1 - d^{*2}/2). \quad (2.2.3.17)$$

This situation also corresponds to the case of flat electronic area detector inclined to the incident beam in a similar way.

Note that Arndt & Wonacott (1977) use  $\nu$  instead of  $\alpha$  here. We use  $\alpha$  and so follow *IT II* (1959). This avoids confusion with the  $\nu$  of Table 2.2.3.1.  $D$  is the crystal to V distance. In the case of the V cassettes of Enraf-Nonius,  $\alpha$  is  $60^\circ$ .

For the case of a cylindrical film or image plate where the axis of the cylinder is coincident with the rotation axis [Fig. 2.2.3.2(c)] then, for  $\gamma$  in degrees,

$$Y_F = \frac{2\pi}{360} D \gamma \quad (2.2.3.18)$$

$$Z_F = D \tan \nu, \quad (2.2.3.19)$$

which becomes

$$Z_F = \frac{D\zeta}{\sqrt{1 - \xi^2}}. \quad (2.2.3.20)$$

Here,  $D$  is the radius of curvature of the cylinder assuming that the crystal is at the centre of curvature.

In the three geometries mentioned here, detector-misalignment errors have to be considered. These are three orthogonal angular errors, translation of the origin, and error in the crystal-to-film distance.

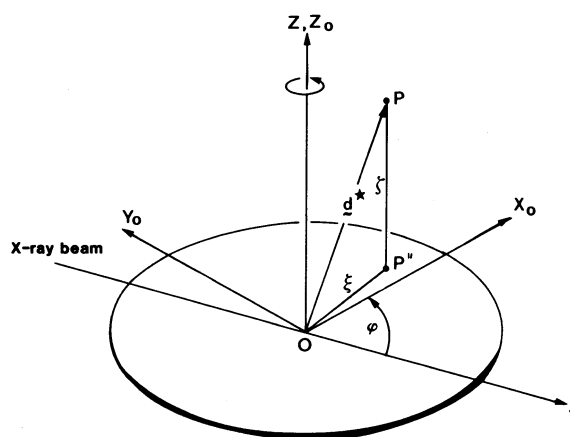


Fig. 2.2.3.3. The rotation method. Definition of coordinate systems. [Cylindrical coordinates of a relp  $P$   $(\xi, \zeta, \varphi)$  are defined relative to the axial system  $X_0Y_0Z_0$  which rotates with the crystal.] The axial system  $XYZ$  is defined such that  $X$  is parallel to the incident beam and  $Z$  is coincident with the rotation axis. From Arndt & Wonacott (1977).

## 2.2. SINGLE-CRYSTAL X-RAY TECHNIQUES

The coordinates  $Y_F$  and  $Z_F$  are related to film-scanner raster units *via* a scanner-rotation matrix and translation vector. This is necessary because the film is placed arbitrarily on the scanner drum. Details can be found in Rossmann (1985) or Arndt & Wonacott (1977).

### 2.2.3.3. Relationship of reciprocal-lattice coordinates to crystal system parameters

The reciprocal-lattice coordinates,  $\zeta, \xi, \gamma, \nu$ , etc. used earlier, refer to an axial system fixed to the crystal,  $X_0Y_0Z_0$  of Fig. 2.2.3.3. Clearly, a given relp needs to be brought into the Ewald sphere by the rotation about the rotation axis. The treatment here follows Arndt & Wonacott (1977).

The rotation angle required,  $\varphi$ , is with respect to some reference 'zero-angle' direction and is determined by the particular crystal parameters. It is necessary to define a standard orientation of the crystal (*i.e.* datum) when  $\varphi = 0^\circ$ . If we define an axial system  $X_0Y_0Z_0$  fixed to the crystal and a laboratory axis system  $XYZ$  with  $X$  parallel to the beam and  $Z$  coincident with the rotation axis then  $\varphi = 0^\circ$  corresponds to these axial systems being coincident (Fig. 2.2.3.3).

The angle of the crystal at which a given relp diffracts is

$$\tan(\varphi/2) = \frac{2y_0 \pm (4y_0^2 + 4x_0^2 - d^{*4})^{1/2}}{(d^{*2} - 2x_0)}. \quad (2.2.3.21)$$

The two solutions correspond to the two rotation angles at which the relp  $P$  cuts the sphere of reflection. Note that  $Y_F, Z_F$  (Subsection 2.2.3.2) are independent of  $\varphi$ .

The values of  $x_0$  and  $y_0$  are calculated from the particular crystal system parameters. The relationships between the coordinates  $x_0, y_0, z_0$  and  $\xi$  and  $\zeta$  are

$$\xi = (x_0^2 + y_0^2)^{1/2}, \quad (2.2.3.22)$$

$$\zeta = z_0. \quad (2.2.3.23)$$

$X_0$  can be related to the crystal parameters by

$$X_0 = Ah. \quad (2.2.3.24)$$

$A$  is a crystal-orientation matrix defining the standard datum orientation of the crystal.

For example, if, by convention,  $a^*$  is chosen as parallel to the X-ray beam at  $\varphi = 0^\circ$  and  $c$  is chosen as the rotation axis, then, for the general case,

$$A = \begin{bmatrix} a^* & b^* \cos \gamma^* & c^* \cos \beta^* \\ 0 & b^* \sin \gamma^* & -c^* \sin \beta^* \cos \alpha \\ 0 & 0 & c^* \end{bmatrix}. \quad (2.2.3.25)$$

If the crystal is mounted on the goniometer head differently from this then  $A$  can be modified by another matrix,  $M$ , say, or the terms permuted. This exercise becomes clear if the reader takes an orthogonal case ( $\alpha = \beta = \gamma = 90^\circ$ ). For the general case, see Higashi (1989).

The crystal will most likely be misaligned (slightly or grossly) from the ideal orientation. To correct for this, the misorientation matrices  $\Phi_x, \Phi_y$ , and  $\Phi_z$  are introduced, *i.e.*

$$\Phi_x = \begin{bmatrix} 1 & 0 & 0 \\ 0 & \cos \Delta\varphi_x & -\sin \Delta\varphi_x \\ 0 & \sin \Delta\varphi_x & \cos \Delta\varphi_x \end{bmatrix} \quad (2.2.3.26)$$

$$\Phi_y = \begin{bmatrix} \cos \Delta\varphi_y & 0 & \sin \Delta\varphi_y \\ 0 & 1 & 0 \\ -\sin \Delta\varphi_y & 0 & \cos \Delta\varphi_y \end{bmatrix} \quad (2.2.3.27)$$

$$\Phi_z = \begin{bmatrix} \cos \Delta\varphi_z & -\sin \Delta\varphi_z & 0 \\ \sin \Delta\varphi_z & \cos \Delta\varphi_z & 0 \\ 0 & 0 & 1 \end{bmatrix}, \quad (2.2.3.28)$$

where  $\Delta\varphi_x, \Delta\varphi_y$ , and  $\Delta\varphi_z$  are angles around the  $X_0, Y_0$ , and  $Z_0$  axes, respectively.

Hence, the relationship between  $X_0$  and  $h$  is

$$X_0 = \Phi_z \Phi_y \Phi_x M A h. \quad (2.2.3.29)$$

### 2.2.3.4. Maximum oscillation angle without spot overlap

For a given oscillation photograph, there is maximum value of the oscillation range,  $\Delta\varphi$ , that avoids overlapping of spots on a film. The overlap is most likely to occur in the region of the diffraction pattern perpendicular to the rotation axis and at the maximum Bragg angle. This is where relp's pass through the Ewald sphere with the greatest velocity. For such a separation between successive relp's of  $a^*$ , then the maximum allowable rotation angle to avoid spatial overlap is given by

$$\Delta\varphi_{\max} = \left[ \frac{a^*}{d_{\max}^*} - \Delta \right], \quad (2.2.3.30)$$

where  $\Delta$  is the sample reflecting range (see Section 2.2.7).  $\Delta\varphi_{\max}$  is a function of  $\varphi$ , even in the case of identical cell parameters. This is because it is necessary to consider, for a given orientation, the relevant reciprocal-lattice vector perpendicular to  $d_{\max}^*$ . In the case where the cell dimensions are quite different in magnitude (excluding the axis parallel to the rotation axis), then  $\Delta\varphi_{\max}$  is a marked function of the orientation.

In rotation photography, as large an angle as possible is used up to  $\Delta\varphi_{\max}$ . This reduces the number of images that need to be processed and the number of partially stimulated reflections per image but at the expense of signal-to-noise ratio for individual spots, which accumulate more background since  $\Delta < \Delta\varphi_{\max}$ . In the case of a CCD detector system,  $\Delta\varphi$  is chosen usually to be

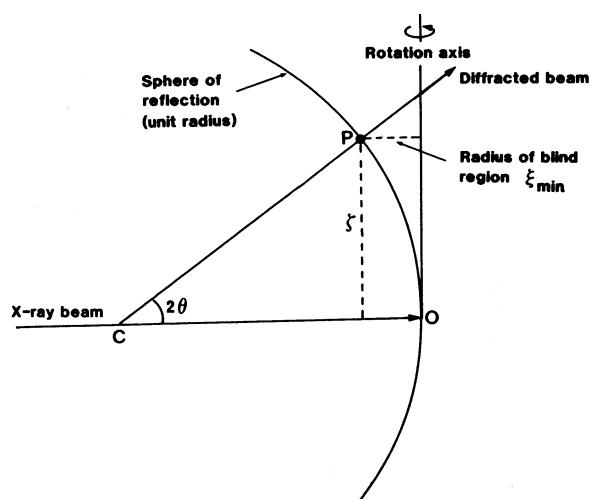


Fig. 2.2.3.4. The rotation method. The blind region associated with a single rotation axis. From Arndt & Wonacott (1977).

## 2. DIFFRACTION GEOMETRY AND ITS PRACTICAL REALIZATION

less than  $\Delta$  so as to optimize the signal-to-noise ratio of the measurement and to sample the rocking-width profile.

The value of  $\Delta$ , the crystal rocking width for a given  $hkl$ , depends on the reciprocal-lattice coordinates of the  $hkl$  relp (see Section 2.2.7). In the region close to the rotation axis,  $\Delta$  is large.

In the introductory remarks to the monochromatic methods used, it has already been noted that originally the rotation method involved  $360^\circ$  rotations contributing to the diffraction image. Spot overlap led to loss of reflection data and encouraged Bernal and Weissenberg to devise improvements. With modern synchrotron techniques, the restriction on  $\Delta\varphi_{\max}$  (equation 2.2.3.30) can be relaxed for special applications. For example, since the spot overlap that is to be avoided involves relp's from adjacent reciprocal-lattice planes, the different Miller indices  $hkl$  and  $h+l, k, l$  do lead in fact to a small difference in Bragg angle. With good enough collimation, a small spot size exists at the detector plane so that the two spots can be resolved. For a standard-sized detector, this is practical for low-resolution data recording. This can be a useful complement to the Laue method where the low-resolution data are rather sparsely stimulated and also tend to occur in multiple Laue spots. Alternatively, a much larger detector can be contemplated and even medium-resolution data can be recorded without major overlap problems. These techniques are useful in some time-resolved applications. For a discussion see Weisgerber & Helliwell (1993). For regular data collection, however, narrow angular ranges are still generally preferred so as to reduce the background noise in the diffraction images and also to avoid loss of any data because of spot overlap.

### 2.2.3.5. Blind region

In normal-beam geometry, any relp lying close to the rotation axis will not be stimulated at all. This situation is shown in Fig. 2.2.3.4. The blind region has a radius of

$$\xi_{\min} = d_{\max}^* \sin \theta_{\max} = \frac{\lambda^2}{2d_{\min}^2}, \quad (2.2.3.31)$$

and is therefore strongly dependent on  $d_{\min}$  but can be ameliorated by use of a short  $\lambda$ . Shorter  $\lambda$  makes the Ewald sphere have a larger radius, *i.e.* its surface moves closer to the rotation axis. At Cu  $K\alpha$  for 2 Å resolution, approximately 5% of the data lie in the blind region according to this simple geometrical model. However, taking account of the rocking width  $\Delta$ , a greater percentage of the data than this is not fully sampled except over very large angular ranges. The actual increase in the blind-region volume due to this effect is minimized by use of a collimated beam and a narrow spectral spread (*i.e.* finely monochromatized, synchrotron radiation) if the crystal is not too mosaic.

These effects are directly related to the Lorentz factor,

$$L = 1/(\sin^2 2\theta - \zeta^2)^{1/2}. \quad (2.2.3.32)$$

It is inadvisable to measure a reflection intensity when  $L$  is large because different parts of a spot would need a different Lorentz factor.

The blind region can be filled in by a rotation about another axis. The total angular range that is needed to sample the blind region is  $2\theta_{\max}$  in the absence of any symmetry or  $\theta_{\max}$  in the case of  $mm$  symmetry (for example).

### 2.2.4. Weissenberg geometry

Weissenberg geometry (Weissenberg, 1924) is dealt with in the books by Buerger (1942) and Woolfson (1970), for example.

#### 2.2.4.1. General

The conventional Weissenberg method uses a moving film in conjunction with the rotation of the crystal and a layer-line screen. This allows:

(a) A larger rotation range of the crystal to be used (say  $200^\circ$ ), avoiding the problem of overlap of reflections (referred to in Subsection 2.2.3.4 on oscillation photography).

(b) Indexing of reflections on the photograph to be made by inspection.

The Weissenberg method is not widely used now. In small-molecule crystallography, quantitative data collection is usually performed by means of a diffractometer.

Weissenberg geometry has been revived as a method for macromolecular data collection (Sakabe, 1983, 1991), exploiting monochromatized synchrotron radiation and the image plate as detector. Here the method is used without a layer-line screen where the total rotation angle is limited to  $\sim 15^\circ$ ; this is a significant increase over the rotation method with a stationary film. The use of this effectively avoids the presence of partial reflections and reduces the total number of exposures required. Provided the Weissenberg camera has a large radius, the X-ray background accumulated over a single spot is actually not serious. This is because the X-ray background decreases approximately according to the inverse square of the distance from the crystal to the detector.

The following Subsections 2.2.4.2 and 2.2.4.3 describe the standard situation where a layer-line screen is used.

#### 2.2.4.2. Recording of zero layer

Normal-beam geometry (*i.e.* the X-ray beam perpendicular to the rotation axis) is used to record zero-layer photographs. The film is held in a cylindrical cassette coaxial with the rotation axis. The centre of the gap in a screen is set to coincide with the zero-layer plane. The coordinate of a spot on the film measured parallel ( $Z_F$ ) and perpendicular ( $Y_F$ ) to the rotation axis is given by

$$Y_F = \frac{2\pi}{360} D \gamma \quad (2.2.4.1)$$

$$Z_F = \varphi/f, \quad (2.2.4.2)$$

where  $\varphi$  is the rotation angle of the crystal from its initial setting,  $f$  is the coupling constant, which is the ratio of the crystal rotation angle divided by the film cassette translation distance, in  $^\circ \text{min}^{-1}$ , and  $D$  is the camera radius. Generally, the values of  $f$  and  $D$  are  $2^\circ \text{min}^{-1}$  and 28.65 mm, respectively.

#### 2.2.4.3. Recording of upper layers

Upper-layer photographs are usually recorded in equi-inclination geometry [*i.e.*  $\mu = -\nu$  in equations (2.2.3.7) and (2.2.3.8)]. The X-ray-beam direction is made coincident with the generator of the cone of the diffracted beam for the layer concerned, so that the incident and diffracted beams make equal angles ( $\mu$ ) with the equatorial plane, where

$$\mu = \sin^{-1} \zeta_n/2. \quad (2.2.4.3)$$

The screen has to be moved by an amount

$$s \tan \mu, \quad (2.2.4.4)$$

where  $s$  is the screen radius. If the cassette is held in the same position as the zero-layer photograph, then reflections produced by the same orientation of the crystal will be displaced

$$D \tan \mu \quad (2.2.4.5)$$